JOURNAL OF AIRCRAFT
Vol. 40, No. 6, November–December 2003

Vortex Generator Installation Drag on an Airplane Near Its Cruise Condition

Kazuhiro Kusunose* and Neng J. Yu†
The Boeing Company, Seattle, Washington 98124

A method is discussed for predicting the drag increment caused by the installation of a blade-type vortex generator (VG) on a transonic-transport airplane. The original Nash and Bradshaw magnification concept of roughness drag is extended to cover compressible flows and then is applied to VG blades to estimate the VG installation drag on an airplane. The drag of a VG blade placed on a wing will be amplified due to the growth of the boundary layer with distance along the wing surface. Nash and Bradshaw showed that the degree of magnification cannot be approximated simply by the ratio of local to freestream dynamic pressure (*q* effect). To demonstrate the magnification effects, some VG installation drag analyses for transonic-transport airplane models are performed using the new magnification factor formula. It can be seen that the agreement between these predicted drag increments and the wind-tunnel test results is good, but the drag increment based on the *q* effect is seriously underestimated.

Introduction

In this paper, we will discuss a new method for predicting the drag increment caused by the installation of a blade-type vortex generator (VG) on a typical transonic-transport airplane wing. Specifically, we will address the drag penalty on the airplane caused by the VG installation as the airplane nears its cruise condition. Nash and Bradshaw[1] pointed out that the increase in profile drag of an airfoil due to an isolated roughness element is, in general, different from the drag of that element measured on a flat plate with the same freestream velocity. They also showed that the drag increment based on the ratio of local to freestream dynamic pressure may be seriously underestimated. Generally, magnification effects are caused not only by the pressure changes along the airfoil surface but also by the boundary-layer development downstream of the roughness element.

Taking the magnification effects into account, we developed a method to predict the installation drag of VG blades on a high-aspect-ratio transonic wing. In this new method, the original Nash and Bradshaw (two-dimensional) magnification concept[1] of roughness drag was extended to a three-dimensional, isolated roughness element by employing a strip theory. Then, the concept was applied to an isolated VG blade placed on a transonic transport airplane wing. During the course of the analysis, only turbulent boundary layers were considered. We will show that the original Nash and Bradshaw concept (for incompressible flows) is also applicable to high-subsonic flows.

The limitation on this method is that the sizes of the VG blades must be small enough so that the VG blades do not affect the pressure distribution over the remainder of the wing. Because VG heights are designed to be at the same order as that of the boundary layer thickness, and because VGs are carefully installed on the wing so that their installations not impact the wing pressure distribution as long as the flow around the wing is attached, this restriction will be naturally satisfied near the model design conditions. The detailed flow changes, in the immediate neighborhood of VG, are not considered here, and the gross effect on the boundary layer is, as discussed in Ref. 1, idealized into a step change in momentum thickness $\Delta\theta_0$.

Presented as Paper 2003-0932 at the AIAA 41st Aerospace Sciences Meeting and Exhibit, Reno, NV, 6 January 2003; received 16 January 2003; revision received 27 February 2003; accepted for publication 27 February 2003.

*Research Engineer, Acoustics and Fluid Mechanics, P.O. Box 3707, MailStop 67-LF, Seattle, WA 98124-2207; kazuhiro.kusunose@boeing.com. Member AIAA.

†Technical Fellow, Enabling Technology and Research, P.O. Box 3707, MailStop 67-LF, Seattle, WA 98124-2207; neng.j.yu@boeing.com.

Spence's[2] Momentum Thickness Equation

Spence[2] solved von Kármán's momentum-integral equation (incompressible) along a two-dimensional turbulent boundary layer

$$\frac{\mathrm{d}\theta}{\mathrm{d}x} + (H+2)\frac{\theta}{U}\frac{\mathrm{d}U}{\mathrm{d}x} = \frac{\tau_w}{\rho U^2} \tag{1}$$

where θ, U, and H are the momentum thickness of the boundary layer, the flow velocity at the outer edge of the boundary layer, and the ratio of displacement to momentum thickness (δ^*/θ), respectively. Here, x is the distance measured along the surface, and τ_w and ρ are the surface shear stress and the density of the fluid. Applying an empirical skin-friction relation for turbulent boundary layers,

$$\tau_w/\rho U^2 \simeq 0.00883(U\theta/\nu)^{-0.2} \tag{2}$$

and approximating $H = \text{const} \simeq 1.5$, Spence looked for an ordinary differential equation in the following form:

$$\frac{\mathrm{d}}{\mathrm{d}x}(\theta^\alpha U^\beta) \sim U^\gamma \tag{3}$$

It was shown in Ref. 2 that the combination of the constants, $\alpha = 1.2$, $\beta = 4.2$, and $\gamma = 4$, or

$$\frac{\mathrm{d}}{\mathrm{d}x}(\theta^{1.2}U^{4.2}) = 0.0106\nu^{0.2}U^4 \tag{4}$$

satisfies von Kármán's momentum-integral equation. Here ν is the kinematic viscosity. Integrating Eq. (4) along the boundary layer from some initial station x_0 to x, one can obtain the growth of the momentum thickness θ with x for the two dimensional turbulent boundary layer in incompressible flow:

$$\theta^{1.2}U^{4.2} = \theta_0^{1.2}U_0^{4.2} + 0.0106\nu^{0.2}\int_{x_0}^{x} U^4\,\mathrm{d}x \tag{5}$$

Although Spence's momentum thickness equation (5) is originally derived for incompressible turbulent boundary layers, it is not

difficult to see that his solution also satisfies the momentum-integral equation for compressible turbulent boundary layers,

$$\frac{\mathrm{d}\theta}{\mathrm{d}x} + (H + 2 - M^2)\frac{\theta}{U}\frac{\mathrm{d}U}{\mathrm{d}x} = 0.00883\left(\frac{U\theta}{\nu}\right)^{-0.2} \tag{6}$$

as long as the following condition

$$H - M^2 \simeq 1.5 \tag{7}$$

is satisfied. Therefore, for the same order of approximation that Spence made for incompressible flows ($H \simeq 1.5$), solution (5) is also valid for attached turbulent boundary layers ($1.5 \leq H \leq 2.5$) up to high-subsonic flow speed ($M \leq 1$). Here, M is the Mach number outside of the boundary layer.

Nash and Bradshaw Magnification Concept[1]

Nash and Bradshaw[1] used Spence's momentum thickness growth equation (5) to estimate the magnification of an isolated roughness drag caused by the pressure gradients along the airfoil surface downstream of the roughness element. A brief summary of their method is given here.

If U_{TE} and θ_{TE} are the velocity outside of the boundary layer and the momentum thickness at the trailing edge on that surface of the airfoil, θ_{TE} can be estimated by Eq. (5),

$$\theta_{\mathrm{TE}}^{1.2}U_{\mathrm{TE}}^{4.2} = \theta_0^{1.2}U_0^{4.2} + 0.0106\nu^{0.2}\int_{x_0}^{x_{\mathrm{TE}}} U^4\,\mathrm{d}x \tag{8}$$

where the subscript zero denotes conditions at some initial station.

Now consider that, due to an isolated roughness element at point $x = x_0$, the momentum thickness increased from θ_0 to $\theta_0 + \Delta\theta_0$. It will be assumed that the step change in momentum thickness due to the roughness element is small compared to the undisturbed momentum thickness, $\Delta\theta_0 \ll \theta_0$, so that the velocities outside the boundary layer remain unchanged. The corresponding change in θ_{TE}, that is, $\Delta\theta_{\mathrm{TE}}$, can be expressed in terms of $\Delta\theta_0$:

$$(\theta_{\mathrm{TE}} + \Delta\theta_{\mathrm{TE}})^{1.2}U_{\mathrm{TE}}^{4.2} = (\theta_0 + \Delta\theta_0)^{1.2}U_0^{4.2} + 0.0106\nu^{0.2}\int_{x_0}^{x_{\mathrm{TE}}} U^4\,\mathrm{d}x \tag{9}$$

Subtracting Eq. (8) from Eq. (9) yields

$$\left[(\theta_{\mathrm{TE}} + \Delta\theta_{\mathrm{TE}})^{1.2} - \theta_{\mathrm{TE}}^{1.2}\right]U_{\mathrm{TE}}^{4.2} = \left[(\theta_0 + \Delta\theta_0)^{1.2} - \theta_0^{1.2}\right]U_0^{4.2} \tag{10}$$

When the definition of the derivative of a function of θ, that is, $F(\theta)$, is

$$F(\theta + \Delta\theta) - F(\theta) \simeq \frac{\mathrm{d}F(\theta)}{\mathrm{d}\theta}\Delta\theta \tag{11}$$

or

$$(\theta + \Delta\theta)^{1.2} - \theta^{1.2} \simeq \frac{\mathrm{d}\theta^{1.2}}{\mathrm{d}\theta}\Delta\theta = 1.2\theta^{0.2}\Delta\theta \tag{12}$$

is kept in mind, Eq. (10) reduces to

$$1.2\theta_{\mathrm{TE}}^{0.2}\Delta\theta_{\mathrm{TE}}U_{\mathrm{TE}}^{4.2} = 1.2\theta_0^{0.2}\Delta\theta_0U_0^{4.2} \tag{13}$$

or

$$\frac{\Delta\theta_{\mathrm{TE}}}{\Delta\theta_0} = \left(\frac{\theta_0}{\theta_{\mathrm{TE}}}\right)^{0.2}\left(\frac{U_0}{U_{\mathrm{TE}}}\right)^{4.2} \tag{14}$$

Because Spence's momentum thickness equation (5) has been extended to high-subsonic flow in the preceding section, remember that this Nash–Bradshaw momentum thickness growth relation (14) is also applicable to high-subsonic flow. Following the method of Squire and Young[3] and Cook[4] for compressible flow, the profile drag of the airfoil is related to the total momentum thickness at the trailing edge. It can be shown that the increase in the drag coefficient of the airfoil, ΔC_D, due to the roughness element is expressed as

$$\Delta C_D = 2\frac{\Delta\theta_{\mathrm{TE}}}{C}\left(\frac{M_{\mathrm{TE}}}{M_\infty}\right)^{(H_{\mathrm{TE}} + H_\infty + 4)/2}\left(\frac{1 + 0.2M_\infty^2}{1 + 0.2M_{\mathrm{TE}}^2}\right)^{(H_{\mathrm{TE}} + H_\infty + 14)/4} \tag{15}$$

where $H_\infty = 1 + 0.4M_\infty^2$ and C represents the chord of the airfoil. In Eq. (15) the value 1.4 has been used for the ratio of specific heats for air, γ. Substituting the relationship between $\Delta\theta_{\mathrm{TE}}$ and $\Delta\theta_0$ given by Eq. (14) into Eq. (15), we can obtain

$$\Delta C_D = 2\frac{\Delta\theta_0}{C}\left(\frac{\theta_0}{\theta_{\mathrm{TE}}}\right)^{0.2}\left(\frac{U_0}{U_{\mathrm{TE}}}\right)^{4.2}\left(\frac{M_{\mathrm{TE}}}{M_\infty}\right)^{(H_{\mathrm{TE}} + 0.4M_\infty^2 + 5)/2} \times \left(\frac{1 + 0.2M_\infty^2}{1 + 0.2M_{\mathrm{TE}}^2}\right)^{(H_{\mathrm{TE}} + 0.4M_\infty^2 + 15)/4} \tag{16}$$

Now, we assume that the values of the drag coefficient of the particular roughness element have been obtained from measurements on a flat plate along which the increase in momentum thickness in the absence of the element could be neglected [$\theta_0 \simeq \theta_{\mathrm{TE}}$ or $(\theta_0/\theta_{\mathrm{TE}})^{0.2} \simeq 1$]. Then, the increase in drag coefficient of the flat plate airfoil is directly proportional to the increase in momentum thickness due to the roughness element. Let $(\theta_0/\theta_{\mathrm{TE}})^{0.2} = 1$, $U_0 = U_{\mathrm{TE}}$, and $M_{\mathrm{TE}} = M_\infty$; Eq. (16) yields

$$\Delta C_D = 2(\Delta\theta_0/C) \equiv C_{Df} \tag{17}$$

where C_{Df} is the increment of drag coefficient of a flat plate airfoil due to the roughness element installation. Then Eq. (16) reduces to

$$\Delta C_D = C_{Df}\left(\frac{\theta_0}{\theta_{\mathrm{TE}}}\right)^{0.2}\left(\frac{U_0}{U_{\mathrm{TE}}}\right)^{4.2}\left(\frac{M_{\mathrm{TE}}}{M_\infty}\right)^{(H_{\mathrm{TE}} + 0.4M_\infty^2 + 5)/2} \times \left(\frac{1 + 0.2M_\infty^2}{1 + 0.2M_{\mathrm{TE}}^2}\right)^{(H_{\mathrm{TE}} + 0.4M_\infty^2 + 15)/4} \tag{18}$$

It is clear that the quantity

$$m = \left(\frac{\theta_0}{\theta_{\mathrm{TE}}}\right)^{0.2}\left(\frac{U_0}{U_{\mathrm{TE}}}\right)^{4.2}\left(\frac{M_{\mathrm{TE}}}{M_\infty}\right)^{(H_{\mathrm{TE}} + 0.4M_\infty^2 + 5)/2} \times \left(\frac{1 + 0.2M_\infty^2}{1 + 0.2M_{\mathrm{TE}}^2}\right)^{(H_{\mathrm{TE}} + 0.4M_\infty^2 + 15)/4} \tag{19}$$

in Eq. (18) represents the magnification of the drag of the roughness element. The drag of the roughness on an airfoil is amplified due to the growth of the (turbulent) boundary layer with distance along the airfoil surface. Combining Eqs. (18) and (19), we finally obtain

$$\Delta C_D = mC_{Df} \tag{20}$$

When the isentropic flow relations and the definition of the speed of sound

$$\frac{M_{\mathrm{TE}}}{M_\infty} = \frac{U_{\mathrm{TE}}}{U_\infty}\frac{a_\infty}{a_{\mathrm{TE}}} = \frac{U_{\mathrm{TE}}}{U_\infty}\left(\frac{1 + 0.2M_{\mathrm{TE}}^2}{1 + 0.2M_\infty^2}\right)^{\frac{1}{2}}$$

are used, the magnification factor given in Eq. (19) can be rewritten

$$m = \left(\frac{\theta_0}{\theta_{\mathrm{TE}}}\right)^{0.2}\left(\frac{U_0}{U_\infty}\right)^{4.2}\left(\frac{U_{\mathrm{TE}}}{U_\infty}\right)^{(H_{\mathrm{TE}} + 0.4M_\infty^2 - 3.4)/2} \times \left(\frac{1 + 0.2M_\infty^2}{1 + 0.2M_{\mathrm{TE}}^2}\right)^{2.5} \tag{21}$$

For incompressible flow (M_{TE}, $M_\infty \to 0$) Eq. (19) reduces to the original Nash–Bradshaw form,[1]

$$m_{\mathrm{incomp}} = (\theta_0/\theta_{\mathrm{TE}})^{0.2}(U_0/U_\infty)^{4.2}(U_{\mathrm{TE}}/U_\infty)^{(H_{\mathrm{TE}} - 3.4)/2} \tag{22}$$

Generalized Magnification Factor for VGs

For the purpose of a crude estimation of VG installation drag on an airplane, we assume that the VG blades installed (in the turbulent boundary-layer region) on a model wing do not affect the pressure distribution over the remainder of the wing. Generally, this pressure condition will be satisfied when the flow around the wing is attached, for example, as the airplane nears its cruise condition, and the VG height h is of the same order as that of the local boundary-layer thickness δ, for example, $h/\delta \leq 2$. Then, when a strip theory is employed, the Nash and Bradshaw (two-dimensional) drag magnification concept[1] can be extended to a three-dimensional small roughness element (such as a trip strip[5] or a VG blade), that is installed on a constant wing section as shown in Fig. 1 (or on a high-aspect-ratio wing). Integrating Eq. (20) along the wing span direction y and using Eq. (17)

$$\int_{y1}^{y2} qC\Delta C_D \,\mathrm{d}y = \int_{y1}^{y2} qCmC_{Df} \,\mathrm{d}y = m\int_{y1}^{y2} qCC_{Df} \,\mathrm{d}y$$

$$= m\int_{y1}^{y2} 2q\Delta\theta_0 \,\mathrm{d}y$$

one can obtain

$$\Delta D = mD_f \tag{23}$$

where ΔD and D_f represent the drag increments of the wing and the equivalent flat plate wing due to an isolated roughness element installed on them. Here q and C are the freestream dynamic pressure defined by $\rho_\infty U_\infty^2/2$ and the local wing chord, respectively.

Similarly, the increment in airplane drag due to the installation of an isolated VG on the wing (VG installation drag), ΔD_{vg}, will be, in general, expressed by

$$\Delta D_{\mathrm{vg}} = M_g D_{f\,\mathrm{vg}} \tag{24}$$

where $D_{f\,\mathrm{vg}}$ denotes the drag increment of the flat plate wing due to a single VG blade installed on it. M_g is a generalized magnification factor that is an extended form of the Nash and Bradshaw's factor, and its derivation will be given shortly. M_g will be a function of the flow variables measured along the wing section on which the VG blade is located (an equivalent two-dimensional wing section as shown in Fig. 2). We define the VG installation drag coefficient of the wing, $\Delta C_{D\,\mathrm{vg}}$, and the drag coefficient of the isolated VG blade placed on the flat plate wing (which has been assumed to be obtained through measuring drag increments of the flat plate wing), $C_{Df\,\mathrm{vg}}$, as

$$\Delta C_{D\,\mathrm{vg}} = \Delta D_{\mathrm{vg}}/qS \tag{25}$$

and

$$C_{Df\,\mathrm{vg}} = D_{f\,\mathrm{vg}}/qS_{\mathrm{vg}} \tag{26}$$

where S and S_{vg} are areas of the model wing and VG blade, respectively. When Eqs. (25) and (26) are substituted into Eq. (24), the

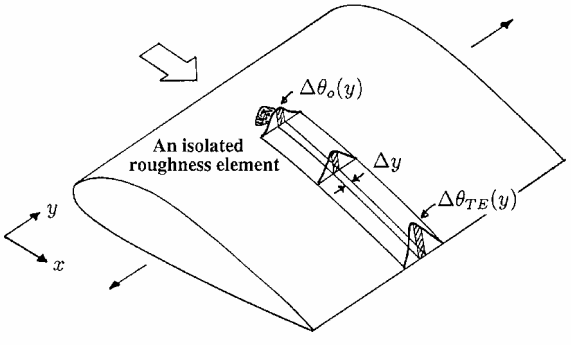

Fig. 1 Extension of two-dimensional drag magnification concept to a three-dimensional roughness element; large aspect ratio (constant wing section) wing, strip theory.

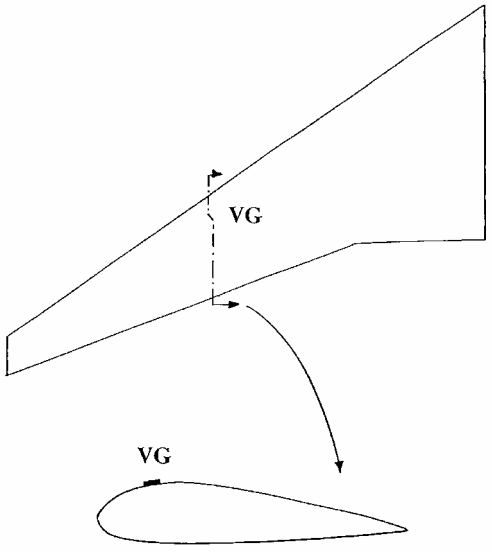

Fig. 2 Wing section on which magnification factor needs to be evaluated; single VG installed on a large aspect ratio wing.

increment in drag coefficient due to a single VG on a wing (single VG installation drag), $\Delta C_{D\,\mathrm{vg}}$, can be expressed by

$$\Delta C_{D\,\mathrm{vg}} = M_g C_{Df\,\mathrm{vg}}(S_{\mathrm{vg}}/S) \tag{27}$$

The derivation of the generalized magnification factor M_g is now shown. For applications of Nash and Bradshaws drag magnification concept[1] to VG blades, note a fundamental difference between a roughness element and a VG blade. For a roughness element, the major part of its drag consists of profile drag, but drag of a VG blade consists of both profile and induced drag. The purpose of installing VG blades on a wing is to generate trailing vortices for promoting boundary-layer mixing along the wing surface. As we reexamine the equations Nash and Bradshaw used in deriving their original drag magnification concept, we can see that they did not consider an induced-drag component, so their concept is valid only for the profile-drag component of the VG blade.

Because the induced drag of a wing (with an elliptic lift distribution) is proportional to the dynamic pressure of the oncoming flow, it is reasonable to assume that the induced drag coefficient of the VG blade placed on a wing will be magnified by the ratio of local to freestream dynamic pressure (q effect). Now approximate $C_{Df\,\mathrm{vg}}$ by the sum of profile and induced drag coefficients of a VG blade installed on a flat plate wing,

$$C_{Df\,\mathrm{vg}} = C_{Df\,\mathrm{vg}P} + C_{Df\,\mathrm{vg}I} \tag{28}$$

The VG installation drag coefficient on the wing, $\Delta C_{D\,\mathrm{vg}}$, can be written as

$$\Delta C_{D\,\mathrm{vg}} = \left[C_{Df\,\mathrm{vg}P}m_{\mathrm{vg}} + C_{Df\,\mathrm{vg}I}(\rho_{\mathrm{vg}}/\rho_\infty)(U_{\mathrm{vg}}/U_\infty)^2\right](S_{\mathrm{vg}}/S)$$

$$= C_{Df\,\mathrm{vg}}\left\{(C_{Df\,\mathrm{vg}P}/C_{Df\,\mathrm{vg}})m_{\mathrm{vg}}\right.$$

$$\left.+[1-(C_{Df\,\mathrm{vg}P}/C_{Df\,\mathrm{vg}})](\rho_{\mathrm{vg}}/\rho_\infty)(U_{\mathrm{vg}}/U_\infty)^2\right\}(S_{\mathrm{vg}}/S) \tag{29}$$

where m_{vg} is Eq. (21), the extension of the Nash and Bradshaw magnification factor. Comparing Eqs. (27) and (29), one can obtain

$$M_g = (C_{Df\,\mathrm{vg}P}/C_{Df\,\mathrm{vg}})m_{\mathrm{vg}}$$

$$+[1-(C_{Df\,\mathrm{vg}P}/C_{Df\,\mathrm{vg}})](\rho_{\mathrm{vg}}/\rho_\infty)(U_{\mathrm{vg}}/U_\infty)^2 \tag{30}$$

Up to this point, we have not discussed the key effects of VGs on the wing boundary layer. The primary purpose of installing VGs on a wing is to promote mixing of the flow along the wing surface to obtain a healthier (but thicker) wing boundary layer. During this mixing process, a good portion of the induced drag of the (well-designed) VG blade will be converted to an additional profile drag

of the wing, resulting in the increase in the skin friction of the wing. Therefore, for the sake of simplicity of the analysis consider a fictitious case in which a VG blade is installed on a (fictitious) inviscid flat plate wing. Then, we assume that the drag increment of the flat plate wing, $C_{Df\,\mathrm{vg}}$, is simply equal to the sum of the profile and induced drag of the VG blade (which is placed on the inviscid flat plate wing):

$$C_{Df\,\mathrm{vg}} \simeq C_{Df\,\mathrm{vg}P} = (C_{Df\,\mathrm{vg}P} + C_{Df\,\mathrm{vg}I})_{\mathrm{invfp}} \tag{31}$$

Finally, we can obtain [from Eq. (30)]

$$M_g \simeq m_{\mathrm{vg}} \tag{32}$$

It is important to note that the extended Nash–Bradshaw magnification factor m_{vg}, given in Eq. (21), is still applicable to the case of the increased skin friction due to the VG installation, as long as the increment of the skin friction is linearly proportional to the original value of the skin friction given in Eq. (2).

Because the actual VG blades are placed in a boundary layer, the effective (wetted) VG area should reduce due to the boundary-layer displacement thickness δ^*. Knowing that $\delta^*/\delta \simeq \frac{1}{7}$ for a typical (flat plate) turbulent boundary layer[6] and that the VG height h is of the same order as that of the local boundary-layer thickness δ, we can estimate the effective VG height as $h - \delta^* \simeq 0.90 \times h$ (i.e., the effective VG area is about $0.90 * S_{\mathrm{vg}}$). Finally, with the help of Eq. (32), Eq. (27) can be written as

$$\Delta C_{D\,\mathrm{vg}} \simeq F m_{\mathrm{vg}} C_{Df\,\mathrm{vg}} (S_{\mathrm{vg}}/S) \tag{33}$$

where F is the correction factor for the effective VG area, and its value should be around 0.9 ($F \simeq 0.9$) for turbulent boundary layers.

Simplified Magnification Factor for VGs

Now, we are going to simplify the magnification factor given by Eq. (21), focusing on its VG applications. The values of the flow velocity U/U_∞ and Mach number M at the VG location and the trailing edge of the wing section (on which the VG is located) can be simply calculated from the known pressure coefficients, C_p on the wing, by using the isentropic flow relations given in Ref. 7, for example, for air, $\gamma = 1.4$,

$$\frac{U}{U_\infty} = \left\{1 - \frac{5}{M_\infty^2}\left[\left(0.7C_pM_\infty^2 + 1\right)^{\frac{2}{7}} - 1\right]\right\}^{\frac{1}{2}} \tag{34}$$

$$M = \left\{2.5\left[\frac{2 + 0.4M_\infty^2}{\left(0.7C_pM_\infty^2 + 1\right)^{\frac{2}{7}}} - 2\right]\right\}^{\frac{1}{2}} \tag{35}$$

However, in general, it is difficult to estimate the (equivalent two-dimensional turbulent) boundary-layer properties θ and H at the VG location and the trailing edge of the wing section (an equivalent two-dimensional airfoil section, as shown in Fig. 2). For the estimation of these values, it is necessary to solve an appropriate two-dimensional turbulent boundary-layer equation for this particular wing section as if it did not have a VG.

For a crude estimation of VG installation drag on a high-aspect-ratio wing near its cruise condition, we assume that VG (chordwise) locations on the wing will be, typically, 10 and 20% chord downstream from the leading edge of the (traditional transonic-transport) wing and that the turbulent boundary layer on the baseline wing (without VGs) is attached. Based on these assumptions and by use of some preliminary results from (turbulent) boundary-layer analyses,[8] it is reasonable to estimate ranges of values of $\theta_{\mathrm{vg}}/\theta_{\mathrm{TE}}$ and H_{TE} to be

$$\theta_{\mathrm{vg}}/\theta_{\mathrm{TE}} = 1/10 \sim 1/30 \tag{36}$$

$$H_{\mathrm{TE}} = 1.4 \sim 1.8 \tag{37}$$

Then the range of $(\theta_{\mathrm{vg}}/\theta_{\mathrm{TE}})^{0.2}$ is

$$0.5065 < (\theta_{\mathrm{vg}}/\theta_{\mathrm{TE}})^{0.2} < 0.6310 \tag{38}$$

To be conservative for the estimation of VG installation drag, we may choose

$$(\theta_{\mathrm{vg}}/\theta_{\mathrm{TE}})^{0.2} \simeq 0.60 \tag{39}$$

$$H_{\mathrm{TE}} \simeq 1.4 \tag{40}$$

When Eqs. (39) and (40) are substituted into Eq. (21), the magnification factor for an isolated VG on a transonic-transport airplane, m_{vg}, can be approximated as

$$m_{\mathrm{vg}} = 0.60\left(\frac{U_{\mathrm{vg}}}{U_\infty}\right)^{4.2}\left(\frac{U_\infty}{U_{\mathrm{TE}}}\right)^{1.0 - 0.2M_\infty^2}\left(\frac{1 + 0.2M_\infty^2}{1 + 0.2M_{TE}^2}\right)^{2.5} \tag{41}$$

For incompressible flow, M_∞, M_{vg} and $M_{\mathrm{TE}} \to 0$, Eq. (41) reduces to the original Nash–Bradshaw formula,[1] then

$$m_{\mathrm{vg-incomp}} = 0.60(U_{\mathrm{vg}}/U_\infty)^{4.2}(U_\infty/U_{\mathrm{TE}}) \tag{42}$$

Note that from Eq. (41) [or Eq. (42)] the magnification m_{vg} occurs when the velocity ratio U_{vg}/U_∞ is greater than unity and that the magnification is larger than the ratio of local to freestream dynamic pressure (q effect), which is proportional to $(U_{\mathrm{vg}}/U_\infty)^2$. Because the velocity ratio appears in Eq. (41) to the power 4.2, the degree of magnification based on the q effect could be seriously underestimated for the VG applications on a lifted wing.

Drag Coefficient of an Isolated VG

To use Eq. (33) for the calculation of installation drag of a single VG blade on a wing, it is necessary to estimate the drag coefficient of the isolated VG blade placed on a flat plate wing, $C_{Df\,\mathrm{vg}}$. As discussed in the preceding section [see Eq. (31)], it has been assumed that the value of $C_{Df\,\mathrm{vg}}$ can be estimated as the sum of the profile and induced drag of the isolated VG blade placed on an inviscid flat plate. In general, aspect ratios of VG blades are small ($\mathrm{AR} \leq 1.0$) and their optimum incidence angle, α_{vg} (Fig. 3), is around 20 deg

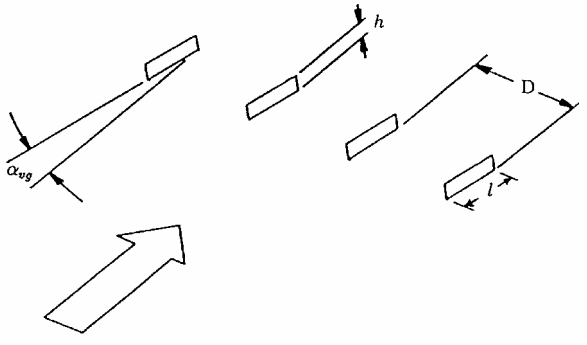

a) Corotating VGs

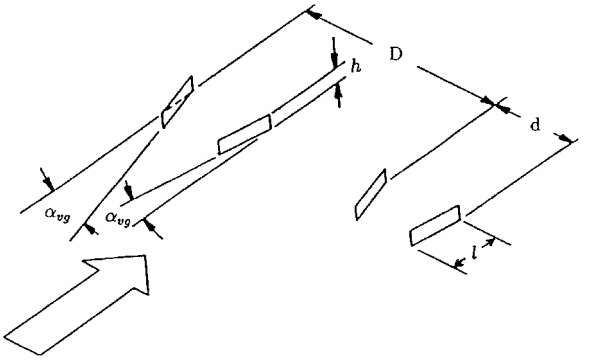

b) Counterrotating VGs

Fig. 3 VG features and notation.

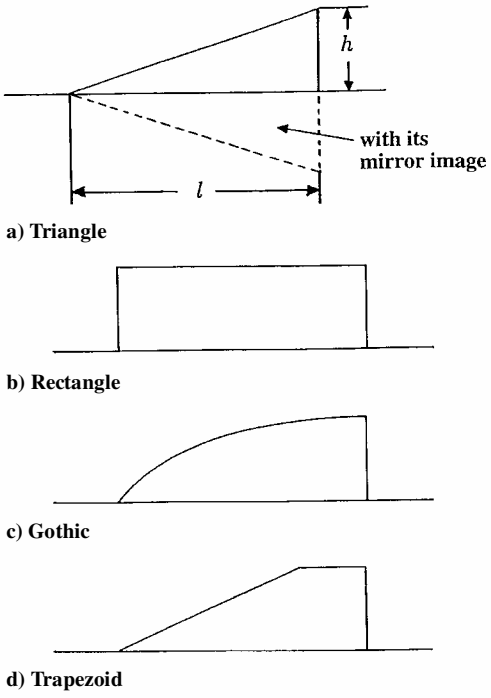

Fig. 4 Typical VG blade planforms.

(Refs. 8–10). When it is known that the flow around a small-aspect-ratio wing with a large incidence angle will separate (generating leading-edge vortices)[11,12] $C_{Df\,\mathrm{vg}}$ can be estimated using a leading-edge-suction analogy developed by Polhamus[13,14] as

$$C_{Df\,\mathrm{vg}} = C_L \tan\alpha_{\mathrm{vg}} \tag{43}$$

where C_L is the lift coefficient of an isolated VG blade with an angle of attack of α_{vg}.

Next, we will discuss how to estimate lift coefficients for two of the commonly used VG shapes; rectangular and triangular (see Fig. 4 for the definitions of VG shapes). For other VG shapes (e.g., Gothic, trapezoidal), their lift coefficients can be approximated by taking a simple average of those from rectangular and triangular VGs.

Triangular-Shaped VG

A triangular-shaped VG blade (with height h and length l), placed on an inviscid flat plate with local flow incidence angle α_{vg} is aerodynamically equivalent to a delta wing (Fig. 4) with a wing span $2h$ and wing area hl and an angle of attack of α_{vg} Polhamus[13,14] has shown (for incompressible flow) that the lift coefficient of a delta wing can be estimated by

$$C_L = K_p \sin\alpha_{\mathrm{vg}} \cos^2\alpha_{\mathrm{vg}} + K_v \cos\alpha_{\mathrm{vg}} \sin^2\alpha_{\mathrm{vg}} \tag{44}$$

where K_p and K_v are functions of aspect ratio of the delta wing. In Refs. 13 and 14, they are plotted (also see Fig. 5). Employing best fit curves for these K_p and K_v data, these parameters can be approximated for small-aspect-ratio wings ($0 \le \mathrm{AR} \le 2$) as

$$K_p = 1.5\mathrm{AR} - 0.2(\mathrm{AR})^2 \tag{45}$$

and

$$K_v = 3.14 + 0.03\mathrm{AR} \tag{46}$$

For example, for a triangular-shaped VG with a length–height ratio of 4 ($l/h = 4$), the aspect ratio of the equivalent delta wing is, $\mathrm{AR} = 1.0$ and let the flow incidence angle be 20 deg ($\alpha_{\mathrm{vg}} = 20$ deg). K_p, K_v, and C_L can be calculated from Eqs. (44–46):

$$K_p = 1.30, \qquad K_v = 3.17, \qquad C_L = 0.741 \tag{47}$$

Then we can calculate $C_{Df\,\mathrm{vg}}$ from Eq. (43):

$$C_{Df\,\mathrm{vg}} = 0.270 \tag{48}$$

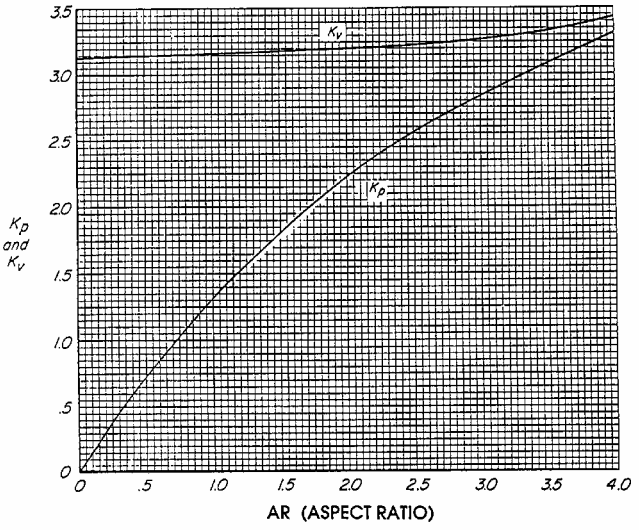

Fig. 5 Variations of K_p and K_v for delta wings.[13]

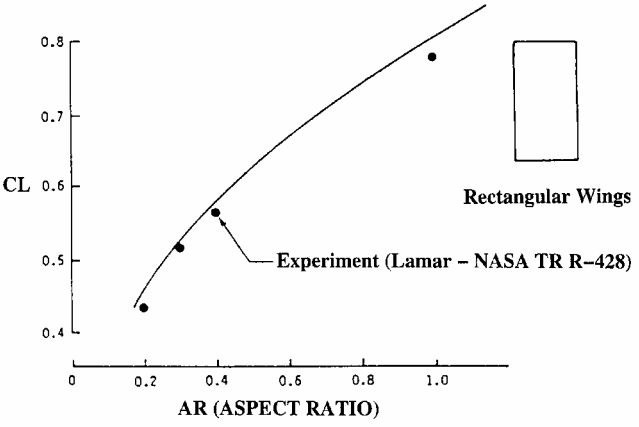

Fig. 6 C_L coefficient for rectangular wings, α = 20 deg and M = 0.2 (Ref. 14).

Rectangular-Shaped VG

Similarly, a rectangular VG (with height h and length l as shown in Fig. 4), placed on an inviscid flat plate with local flow angle α_{vg} (see Fig. 3), is equivalent to a rectangular wing with a wing span $2h$ and wing area $2hl$ and an angle of attack α_{vg}. Johnson et al.[15] calculated and plotted C_L for a rectangular wing with a small aspect ratio ($0.2 \le \mathrm{AR} \le 1.1$) and an angle of attack of 20-deg (see Fig. 6). Using a best-fit curve the plot in Fig. 6, lift coefficients of small-aspect-ratio rectangular wings can be approximated as a function of aspect ratio:

$$C_L = 0.3117 + 0.6850\mathrm{AR} - 0.2167(\mathrm{AR})^2 \tag{49}$$

When the wing incidence angle α_{vg} is not exactly 20 deg, C_L can be estimated using either the experimental or analytical results given in Ref. 16, or we could simply use a linear extrapolation (for a good estimation)

$$C_L = (C_L)_{\alpha_{\mathrm{vg}}=20}(\alpha_{\mathrm{vg}}/20) \tag{50}$$

where $(C_L)_{\alpha_{\mathrm{vg}}=20}$ is the C_L calculated from Eq. (49).

Finally, using Eqs. (50) and (43), $C_{Df\,\mathrm{vg}}$ for a rectangular-shaped VG can be calculated. For example, C_L and $C_{Df\,\mathrm{vg}}$ for a rectangular VG with a length–height ratio of 4 ($l/h = 4$, hence, the 0.5 aspect ratio of the equivalent rectangular wing) with its 20 deg incidence angle will be

$$C_L = 0.600, \qquad C_{Df\,\mathrm{vg}} = 0.218 \tag{51}$$

Gothic and Trapezoidal-Shaped VGs

For a Gothic or Trapezoidal shaped VG (Fig. 4), C_L can be estimated using the C_L of both triangular- and rectangular-shaped VGs. As an example, for a Gothic-shaped VG with length–height ratio of $4(l/h = 4)$ with an incidence angle of 20 deg, an approximated lift coefficient would be the simple average of the C_L calculated from the triangular- and rectangular-shaped VGs [referring to the C_L from Eqs. (47) and (51)]

$$C_L \simeq (0.741 + 0.600)/2 = 0.671 \tag{52}$$

and its drag coefficient $C_{Df\,\mathrm{vg}}$ would be

$$C_{Df\,\mathrm{vg}} = 0.671 \tan 20 = 0.244 \tag{53}$$

Mach Number Effect on $C_{Df\,\mathrm{vg}}$

Generally, lift and drag coefficients of an isolated VG blade (placed on an inviscid flat plate) are functions of the freestream Mach number. Because the current C_L and $C_{Df\,\mathrm{vg}}$ formulas were derived for incompressible flows,[13–15] it is necessary to consider the compressible flow effects on them for VG applications to transonic-transport airplanes.

In Ref. 17, K_p and K_v, used for the C_L estimation of triangular-shaped VGs, were extended to cover compressible flows, and an evaluation on this extended leading-edge suction analogy was given. Additional comparisons between theoretical and experimental values of lift and drag coefficients were made for small-aspect-ratio wings in Refs. 16 and 18, showing that the reduction in lift and drag with the increasing freestream Mach number was well predicted by using the extended leading-edge suction analogy given in Ref. 17. Because those theoretical and experimental results given in Refs. 16–18 show that both the lift and drag coefficients are nearly independent of Mach number up to a transonic flow speed, it is reasonable to approximate them to be independent of Mach number throughout the subsonic and transonic flow range. For the sake of simplicity, we use the incompressible C_L and $C_{Df\,\mathrm{vg}}$ formulas given by Eqs. (43–46) and (49) for the current VG applications.

VG Installation Drag Estimation

In this section we will demonstrate how to estimate the VG installation drag on a transonic-transport airplane using the airplane's given wing pressure distribution. The formula to use for the drag estimation of a single VG installation is Eq. (33), where m_{vg} and $C_{Df\,\mathrm{vg}}$ are defined in Eqs. (41) [or Eq. (21) for the exact value of m_{vg}] and (31), respectively. If the chosen reference wing area is a half of the (entire) model wing area, $\Delta C_{D\,\mathrm{vg}}$ represents the drag (coefficient) increment due to a single VG installed on one side of the model wing (two VGs would have been installed on the entire model wing.)

For the calculation of the magnification factor m_{vg}, it is necessary to know the values of U/U_∞ and M at both the VG and trailing-edge locations of the wing section on which the VG is (or will be) installed. When the pressure distribution is known at this wing section (obtained from experiments or computational fluid dynamics analyses, etc.), these values can be calculated from Eqs. (34) and (35). For demonstration, we chose a rectangular VG blade with dimensions of $l = 3.78$ in. (9.60 cm) and $h = 0.94$ in. (2.39 cm) $(l/h \simeq 4)$, and we assumed that its incidence angle was about 20 deg and that VGs will be placed on each side of a transonic airplane wing on which $S = 4605$ ft^2 (427.78 m^2). Arbitrarily setting the VGs spanwise and chordwise locations to be 70 and 15%, respectively, and the airplane's operating Mach number and its Reynolds number to be $M_\infty = 0.83$ and $Re = 45 \times 10^6$, respectively, we proceeded to estimate the VG installation drag.

When the pressure distribution of the wing section on which a VG is to be installed is known (e.g., Fig. 7), the pressure coefficients at the VG and the trailing-edge locations can be found for example, $C_{p\,\mathrm{vg}} \simeq -1.0$ and $C_{p\,\mathrm{TE}} \simeq 0.1$, respectively. Then, from Eqs. (34) and (35), we can obtain $U_{\mathrm{vg}}/U_\infty = 1.498$,

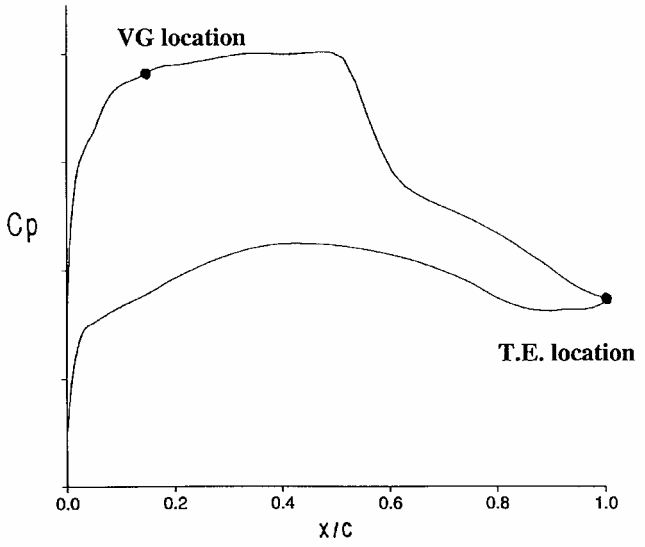

Fig. 7 Sample pressure distribution, Mach 0.83 pressure data, cruise alpha.

$U_{\mathrm{TE}}/U_\infty = 0.950$, $M_{\mathrm{vg}} = 1.366$, and $M_{\mathrm{TE}} = 0.783$. Finally, the (simplified) magnification factor m_{vg} will be calculated from Eq. (41),

$$m_{\mathrm{vg}} = 0.60(1.498)^{4.2}\left(\frac{1}{0.950}\right)^{1.0-0.2(0.83)^2}\left[\frac{1+0.2(0.83)^2}{1+0.2(0.783)^2}\right]^{2.5} = 3.543 \tag{54}$$

When $C_{Df\,\mathrm{vg}} = 0.218$ is found from Eq. (51) for the rectangular VG of $l/h = 4$, and (for our demonstration) $S_{\mathrm{vg}} = 3.78 * 0.94$ (in.^{2}) and $S = 4605/2$ (ft^2) for one side of the wing, VG installation drag will be estimated from Eq. (33),

$$\Delta C_{D\,\mathrm{vg}} = 0.90 * 3.543 * 0.218 * \frac{3.78 * 0.94}{(4605/2) * 12^2} = 0.7449 * 10^{-5} \tag{55}$$

This $\Delta C_{D\,\mathrm{vg}}$ represents the single-VG installation drag on one side of a wing (or two VGs on the entire model wing). For a case of multiple VGs installed on a wing, we can repeat the processes discussed in this section for each individual VG blade, and the total VG installation drag on the airplane will be the sum of the drag from each individual VG installation.

Results and Discussion

Some NASA Ames Research Center high-Reynolds-number test results for VG applications on a transonic-transport configuration[8] were analyzed using the original Nash–Bradshaw[1] (incompressible) magnification factor concept [given by Eq. (22)]. To demonstrate the magnification effects, predicted VG installation drag based on several different methods (indicated by the lines in Fig. 8) was compared with the tunnel balance data (symbols in Fig. 8). With reference to Eq. (33), the y axis in Fig. 8, $\Delta C_D/(S_{\mathrm{vg}}/S)$, represents the value of $C_{Df\,\mathrm{vg}} * F * m_{\mathrm{vg}} *$ number of VGs. If a single VG is installed on an (fictitious) inviscid flat plate wing ($q_{\mathrm{vg}} = q_\infty$ and $F = 1$), the value of the magnification factor will be one, and $\Delta C_D/(S_{\mathrm{vg}}/S) = C_{Df\,\mathrm{vg}}$. When the q effect is considered, the drag increment of the wing (due to the single-VG blade) will be $C_{Df\,\mathrm{vg}} * q/q_\infty$. Then, if the boundary-layer magnification factor is applied to it, it becomes $C_{Df\,\mathrm{vg}} * m_{\mathrm{vg}}$. Note that the drag increments based on the q effect were seriously underestimated. However, the drag increments predicted by using the magnification factor agreed very well with the wind-tunnel data. Also note that the correction of effective VG area due to the displacement thickness of the turbulent boundary layer $\delta^*(F \simeq 0.9)$ yielded an additional improvement.

Currently, some VG installation drag analyses for a transonic-transport, 2.7% scale model in the National Transonic Facility (NTF)

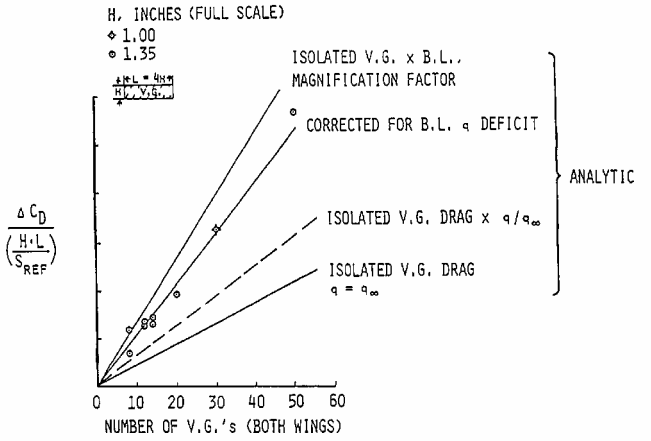

Fig. 8 NASA Ames Research Center high Reynolds number test results for a transonic-transport airplane, VG drag with $C_L = 0.5$, $Re = 14 \times 10^6$, and $(x/c)_{vg} = 0.20$.

at NASA Langley Research Center are performed using the simplified magnification factor formula.[19] In the NTF, three different sizes of rectangular VGs (with length–height ratio of 4) corresponding to different wind-tunnel Reynolds numbers ($3 * 10^6$, $10.3 * 10^6$, and $40 * 10^6$) were tested at several transonic speeds ($M_\infty = 0.70$, 0.84, and 0.87) (Ref. 20). The general agreement between the predicted VG installation drag and the drag measured in the wind tunnel is good. The discussions on the VG analysis are, unfortunately, not given here, because specific results of this NTF test are considered proprietary.

Conclusions

To predict the VG installation drag on transonic-transport airplanes, the Nash–Bradshaw[1] magnification concept of roughness drag was extended for compressible flows and used for the estimation of the VG installation drag. Note that the magnification occurs when the velocity ratio (at the VG location) U_{vg}/U_∞ is greater than unity and that the magnification is larger than the ratio of local to freestream dynamic pressure (q effect), which is proportional to $(U_{vg}/U_\infty)^2$. Because the velocity ratio appears in the magnification factor to the power of 4.2, the magnification based on the q effect does not even qualify as a close approximation. To demonstrate the current VG installation drag-prediction capability, some VG installation drag analyses for transonic transport airplanes were performed, and these results were compared to wind-tunnel and flight-test results.[19]

Acknowledgments

We would like to thank J. D. McLean, E. N. Tinoco, and M. M. Curtin of Boeing Enabling Technology and Research for many valuable discussions and comments over the course of developing the current method. Further thanks are extended to E. N. Tinoco for giving us the opportunity to work on this problem.

References

[1] Nash, J. F., and Bradshaw, P., "The Magnification of Roughness Drag by Pressure Gradients," *Journal of the Royal Aeronautical Society*, Vol. 71, Jan. 1967, pp. 44–46.

[2] Spence, D. A., "The Development of Turbulent Boundary Layers," *Journal of the Aeronautical Sciences*, Vol. 23, Jan. 1956, pp. 3–15.

[3] Squire, H. B., and Young, A. D., "The Calculation of the Profile Drag of Aerofoils," Aeronautical Research Committee Reports and Memoranda 1838, Aeronautical Research Council, London, Nov. 1937.

[4] Cook, T. A., "Measurements of the Boundary Layer and Wake of Two Aerofoil Sections at High Reynolds Numbers and High-Subsonic Mach Numbers," Aeronautical Research Council Reports and Memoranda 3722, Aeronautical Research Council, London, June 1971.

[5] Witkowski, D. P., Loh, K. C., and Kusunose, K., "Trip Drag Estimation Method Based on Magnification Factor Concept," Boeing Coordination Sheet, ER&D-BBAA6-C2002-033, July 2002.

[6] Cebeci, T., and Bradshaw, P., *Momentum Transfer in Boundary Layers*, McGraw–Hill, New York, 1977, pp. 18–20.

[7] Liepmann, H. W., and Roshko, A., *Elements of Gasdynamics*, Wiley, New York, 1956, pp. 53–55.

[8] Nagel, A. L., Tinoco, E. N., and Kusunose, K., "'Vortex Generators, Summary of Recent Data' (view foils) in Vortex Generator Design Guide Study," Vol. 3, Sec. 13, Aerodynamic Technology and Development Job Book System, The Boeing Co., Seattle, WA, March 1982.

[9] Pearcey, H. H., "Shock-Induced Separation and Its Prevention by Design and Boundary Layer Control," Boundary Layer and Flow Control, edited by G. V. Lachmann, Vol. 2, Pergamon, New York, 1961, pp. 1166–1344.

[10] Mabee, T., "Vortex Generator Aerodynamic Design Guidelines for the Mitigation of Shock-Induced Separation," Document D6-81501TN, The Boeing Co., Seattle, WA, Feb. 1995.

[11] Jones, R. T., and Cohen, D., *High Speed Wing Theory*, Princeton Univ. Press, Princeton, NJ, 1960, pp. 108–110.

[12] Kuethe, A. M., and Chow, C. Y., *Foundation of Aerodynamics: Bases of Aerodynamic Design*, 3rd ed., Wiley, New York, 1976, pp. 413, 414.

[13] Polhamus, E. C., "A Concept of the Vortex Lift of Sharp-Edge Delta Wings Based on a Leading-Edge-Suction Analogy," NASA TN D-3767, Dec. 1966.

[14] Polhamus, E. C., "Application of the Leading-Edge-Suction Analogy of Vortex Lift to the Drag due to Lift of Sharp-Edge Delta Wings," NASA TN D-4739, Aug. 1968.

[15] Johnson, F. T., Tinoco, E. N., Lu, P., and Epton, M. A., "Three-Dimensional Flow over Wings with Leading-Edge Vortex Separation," *AIAA Journal*, Vol. 18, No. 4, 1980, pp. 367–380.

[16] Lamar, J. E., "Extension of Leading-Edge-Suction Analogy to Wings with Separated Flow around the Side Edges at Subsonic Speeds," NASA TR R-428, Oct. 1974.

[17] Polhamus, E. C., "Prediction of Vortex-Lift Characteristics by a Leading-Edge-Suction Analogy," *Journal of Aircraft*, Vol. 8, No. 4, 1971, pp. 193–199.

[18] Davenport, E. E., "Aerodynamic Characteristics of Three Slender Sharp-Edge 74° Swept Wings at Subsonic, Transonic, and Supersonic Mach Numbers," NASA TN D-7631, Aug. 1974.

[19] Kusunose, K., "Estimation of Vortex Generator Installation Drag on a Transonic-Transport Airplane Near Its Cruise Condition," Document D6-82707, The Boeing Co., Seattle, WA, Aug. 2001.

[20] Curtin, M. M., Bogue, D. R., Om, D., Rivers, S. M. B., Pendergraft, O. C., Jr., and Wahls, R. A., "Investigation of Transonic Reynolds Number Scaling on a Twin-Engine Transport (Invited)," AIAA Paper 2002-0420, Jan. 2002.

[21] LaPrete, R. D., "Vortex Generator Drag Calculation for Wings," Coordination Sheet AERO-B-BBA6-C01-1621, The Boeing Co., Seattle, WA, Dec. 2001.